Journal of Photochemistry and Photobiology 11 (2022) 100122

Contents lists available at ScienceDirect

Journal of Photochemistry and Photobiology

journal homepage: www.sciencedirect.com/journal/journal-of-photochemistry-and-photobiology

Inhibitory effects of calcium or magnesium ions on PDI

Daniel Bernhard Eckl [a,*], Nicole Landgraf [a], Anja Karen Hoffmann [a], Laura Schottenhaml [a], Julia Dirscherl [a], Nina Weber [a], Stefanie Susanne Eben [a], Pauline Bäßler [b], Anja Eichner [b], Harald Huber [a], Wolfgang Bäumler [b]

[a] Department of Microbiology, University of Regensburg, Regensburg, Germany
[b] Clinic and Polyclinic of Dermatology, University Hospital Regensburg, Regensburg, Germany

ARTICLE INFO

Keywords:
Photodynamic inactivation
Divalent ions
Magnesium
Calcium
Photosensitizers

ABSTRACT

Photodynamic inactivation of microorganisms (PDI) finds use in a variety of applications. Several studies report on substances enhancing or inhibiting PDI. In this study, we analyzed the inhibitory potential of ubiquitous salts like $CaCl_2$ and $MgCl_2$ on PDI against *Staphylococcus aureus* and *Pseudomonas aeruginosa* cells using five cationic photosensitizers methylene blue, TMPyP, SAPYR, FLASH-02a and FLASH-06a.

TMPyP changed its molecular structure when exposed to $MgCl_2$, most likely due to complexation. $CaCl_2$ substantially affected singlet oxygen generation by MB at small concentrations. Elevated concentrations of $CaCl_2$ and $MgCl_2$ impaired PDI up to a total loss of bacterial reduction, whereas $CaCl_2$ is more detrimental for PDI than $MgCl_2$. Binding assays cannot not explain the differences of PDI efficacy. It is assumed that divalent ions tightly bind to bacterial cells hindering close binding of the photosensitizers to the membranes. Consequently, photosensitizer binding might be shifted to outer compartments like teichoic acids in Gram-positives or outer sugar moieties of the LPS in Gram-negatives, attenuating the oxidative damage of susceptible cellular structures.

In conclusion, $CaCl_2$ and $MgCl_2$ have an inhibitory potential at different phases in PDI. These effects should be considered when using PDI in an environment that contains such salts like in tap water or different fields of food industry.

1. Introduction

PDI nowadays has a wide range of possible applications. There is plenty of experimental applications in development for example in wastewater treatment [1–8], implementation in antimicrobial coatings [9,10], lowering the microbial load of food and crops [11–14], decolonization of human skin [15] or in dentistry [16–18]. Furthermore, Majiya and colleagues demonstrated sunlight driven water disinfection with a porphyrin immobilized in a chitosan membrane. The researchers successfully reduced the bacterial load by three orders of magnitude and therefore demonstrate a cost-efficient and sustainable method for drinking water disinfection [19].

The herein cited examples for applied PDI make use of several photosensitizer classes, ranging from well-known photosensitizers such as methylene blue (MB), porphyrins (5,10,15,20-Tetrakis(1-methyl-4-pyridinio)-porphyrin tetra(p-toluene sulfonate, briefly called TMPyP), new substances that exclusively produce singlet oxygen (SAPYR [20]) to curcumins or flavins (FLASH-02a and FLASH-06a [21]). Especially curcumins are considered safe for food applications [12].

The efficacy of PDI is frequently studied under laboratory conditions using media like PBS, which are rather uncommon when considering PDI applications under real life conditions. Thus, when comparing PDI efficacies of environmental photodynamic applications with ones from *in vitro* laboratory studies, it is not surprising that the results of such studies seem to diverge tremendously in some cases.

As mentioned, several fields of application are conceivable for photodynamic inactivation, in which a wide variety of substances, including divalent ions, will inevitably be present. An example of a potential future application outside the laboratory is the antimicrobial treatment of water [19,22–24]. Exemplarily for tap water, water hardness is calculated based on the concentration of calcium carbonate and has the following definition according to the US Geological Service. A concentration of 0 – 0.6 mmol l^{-1} is considered as soft water, 0.61 – 1.2 mmol l^{-1} moderately hard water, 1.21 – 1.80 mmol l^{-1} hard water, and above 1.8 mmol l^{-1} very hard water [25]. In Germany, water hardness is divided in three categories termed soft for <1.5 mmol l^{-1}, medium from

* Corresponding author at: Daniel B. Eckl, Department of Microbiology, University of Regensburg, Universitätsstraße 31, 93053 Regensburg.
E-mail address: Daniel.eckl@ur.de (D.B. Eckl).

https://doi.org/10.1016/j.jpap.2022.100122
Received 9 February 2022; Received in revised form 28 March 2022; Accepted 26 April 2022
Available online 29 April 2022

1.5 to 2.5 mmol l^{-1} and hard is > 2.5 mmol l^{-1} measured as total $CaCO_3$ [26]. Worldwide, concentrations of calcium and magnesium ions vary greatly depending on the geological background the water originates from. The concentration of calcium ions in drinking water derived from ground water generally ranges from about 0.025 mmol l^{-1} to 2.5 mmol l^{-1} with values reported up to nearly 10 mmol l^{-1} [27–33]. Magnesium in drinking water is found all around the world and varies greatly depending on the geographical region. Studies from Sweden found magnesium ion concentrations in drinking water of around 0.065 up to 0.62 mmol l^{-1} [34–36], reports from Norway mentioned concentrations up to 0.1 mmol l^{-1} [37] with a median of around 0.2 mmol l^{-1} [38]. Research from England measured values up to 4.56 mmol l^{-1} [39] and another study from South-Africa reported on magnesium concentrations up to 2 mmol l^{-1} [40].

Another application of PDI is the inactivation of microorganisms in food production and processing [41–43]. Approaches of applying PDI towards milk [44] should be taken into focus as divalent ions are inevitably present. The calcium content of milk depends to a certain extent also on the breed of the milked cow [45] or the diet of the cow itself [46]. The various milks commercially available today have quite similar calcium concentrations between 29.5 and 31.56 mmol l^{-1}. Yoghurt on the other hand varies in a range of 34.62 to 45.62 mmol l^{-1}. The calcium concentration of raw cheese varies between 98.02 to 299.40 mmol l^{-1} [47].

A future promising approach is the treatment of the human skin based on photosensitizer solutions. Although this has been proven to show good initial results, the obtained inactivation values are still lower than when experiments are conducted in controlled liquid environment with H_2O. For example, within this study, good efficacy of at least 6 orders of magnitude was achieved for SAPYR for 0.72 J cm^{-2} and 50 μmol l^{-1}. However, on *ex vivo* skin experiments at least 100 μmol l^{-1} were applied in combination with at least 30 J cm^{-2} in order to achieve sufficient inactivation [15]. Similar findings were reported by another research group where harsher parameters for efficient inactivation had to be applied in an *in vivo* model [48]. The differences in the efficacy of these experiments are to a certain extent based on slight experimental differences. However, experiments on skin in general or sweat in particular are by no means similar to pure water. Much more, they resemble complex environments with a variety of substances, even in literature, the found compositions vary greatly [49,50]. Sweat also contains various amounts of calcium and magnesium that inhibit the PDI at least to a certain extent.

Even though the commercial application of PDI in various environments is one of the major aims, it is frequently not sufficiently explored whether or to which extent various ubiquitous substances in these environments may hamper PDI efficacy when using such photosensitizers. Among others, up to date the effects of abundant substances such as calcium or magnesium ions or complex biological molecules remain mostly uninvestigated. Of course, it is known for some photosensitizer that certain chemicals inhibit [21,51] or enhance [52–54] the photodynamic process. One of the most prominent molecules in this context is sodium azide acting as a potent physical singlet oxygen quencher [51]. In contrast, there are also studies investigating on effects that promote the photodynamic action in presence of sodium azide [54]. Furthermore, it was recently shown that carbonate and phosphate ions, which are two prominent molecules in most environments, have detrimental effects on the chemical structure of flavin based photosensitizers [21]. Additionally, some research data concerning the photodynamic treatment of milk suggested that calcium and magnesium ions pose some issues in efficacy [44].

Therefore, we hypothesize that ubiquitous bivalent ions might affect the photodynamic process at different stages. In this study, we investigated five different cationic PS with various chemical structures such as a porphyrin, a phenothiazine, two flavins and a phenalenone. The biocidal potential of the different photosensitizers towards several bacteria was evaluated under the influence of various aqueous solutions containing calcium and magnesium in ascending concentrations resembling concentrations found in possible areas of future applications.

2. Material and Methods

2.1. Photosensitizers

Methylene blue was purchased from SERVA Electrophoresis GmbH with a minimum dye content of 96%. Methylene blue has a singlet oxygen quantum yield of around 0.50 depending on the applied measurement method [55], providing a mixture of ROS and singlet oxygen that is generated. TMPyP was brought from Sigma-Aldrich with a minimum dye content of 97%. The quantum yield of the porphyrin based photosensitzer is around 0.77 [56], producing chiefly singlet oxygen with minor amounts of other ROS. Besides, an exclusive singlet oxygen producing photosensitizer shortly called SAPYR with a quantum yield of 0.99 [20] was purchased from the TriOptoTec GmbH, the chemical structure of the molecules has been published elsewhere [21]. Additionally, two different flavin based photosensitizers were included with a quantum yield of around 0.75 that was also purchased from TriOptoTec GmbH. In general, all light sensitive parts of the procedures were conducted at low light conditions with a maximum radiant flux of 55 μW cm^{-2} as described elsewhere [57].

2.2. Bacteria

The used bacterial strains were obtained from the German Collection of Microorganisms and cell culture lines DSMZ (Braunschweig, Germany). As a Gram-positive representative *Staphylococcus aureus* F-182 (DSM 13661) was used. The strain was derived from a clinical isolate from Kansas and exhibits resistance towards methicillin and oxacillin, therefore also considered as MRSA. The Gram-negative organism tested in this study was *Pseudomonas aeruginosa* Boston 41501 (DSM 1117) initially isolated from a blood culture. As universal culture medium Mueller-Hinton-Bouillon [58] was used on which the bacteria grew over night at 37°C at 100 rpm.

2.3. Ionic solutions

Stock solutions of calcium chloride ($CaCl_2$) and magnesium chloride ($MgCl_2$) were prepared with stock concentrations of 150, 15, 1.5 and 0.15 mmol l^{-1}. As a solvent and control served ultra-pure H_2O with a conductance of 0.056 μS cm^{-1} (Milli-Q® Water Treatment System, Merck KGaA, Darmstadt, Germany). The stock solutions were stored in plug-sealed, gas tight glass serum bottles under nitrogen atmosphere in the dark at room temperature. pH was adjusted to 7 using HCl or NaOH. $CaCl_2$ as well as $MgCl_2$ were purchased from Carl Roth GmbH + Co. KG (Karlsruhe, Germany) in analytical grade.

2.4. Light source

For TMPyP, SAPYR, FLASH-02a and FLASH-06a a blue light source (blue_v, Waldmann GmbH, Villingen-Schwenningen, Germany) was used, while MB was irradiated under a red light source (PDT 1200, Waldmann GmbH, Villingen-Schwenningen, Germany). The applied irradiance for the blue light source was 18 mW cm^{-2} and for the red light source 20 mW cm^{-2}. The final radiant exposure depended on the time of the application and is represented the product of the applied irradiance in W cm^{-2} times the application time in s resulting in J cm^{-2}, which are the values given throughout the following.

2.5. Spectroscopic analysis

To investigate if aqueous solutions alter the chemical structure of the used photosensitizers, spectroscopic analysis was performed from 300 to 700 nm in a photometer (BMG Labtec, Ortenberg, Germany) with a 96-

well microtiter plate (SARSTEDT AG & Co. KG, Nümbrecht, Germany). To rule out light induced reactions, the spectra were recorded before and after illumination with an appropriate light source with defined energy up to 5.4 J cm^{-2}. Each reaction was composed out of a total volume of 200 µl with PS concentrations ranging from 0 to 50 µmol l^{-1} and ionic solutions in concentrations of up to 75 mmol l^{-1}. The obtained transmission was then plotted with OriginLab 2019b (Northampton, USA).

2.6. Singlet oxygen production

To evaluate singlet oxygen production in qualitative manners, DPBF (1,3-Diphenylisobenzofurane) assays were carried out. DPBF was purchased from Sigma-Aldrich with a minimum dye content of 97%. DPBF reactions were composed in total as follows: a total volume of 200 µl contained either no PS (internal reference) or 1 to 50 µmol l^{-1} PS, 75 mmol l^{-1} $CaCl_2$ or $MgCl_2$ and 500 µmol l^{-1} DPBF which was dissolved in analytic grade ethanol. Assays were conducted as triplicates and measured after a total applied energy of 0, 0.018, 0.036, 0.054, 0.072, 0.09 and 0.18 J cm^{-2} with either the blue_v light source or the respective red light source. DPBF fluorescence was then measured utilizing a fluorescence plate reader from BMG Labtech with the excitation wavelength of 411 nm and emission detection at 451 nm. Values obtained for the internal reference (DPBF without PS) were set to 1, relative fluorescence was calculated as rations to the internal reference and the sample (DPBF with PS) and displayed in per cent using OriginLab 2019b software.

2.7. Evaluation of the logarithmic bacterial reduction

Bacterial cultures were harvested via centrifugation at 13,000 x g for 7 min. Afterwards, OD_{600} was adjusted to 0.6 with a cell density meter (Ultrospec 10, Ammersham Biosciences, Little Chalfont, UK). 1 ml of the cell suspension was transferred to 1.5 ml reaction tubes and centrifuged at 13,000 x g for 7 min. Supernatant was discarded and the remaining pellet was washed in H_2O three times. After the last washing step, the cells were mixed with 1 ml of either $CaCl_2$, $MgCl_2$ or H_2O in concentrations of 75 to 0.75 mmol l^{-1}. 25 µl of the bacterial cell suspension were mixed with the same volume of PS solutions in ascending concentrations, incubated for 10 min at room temperature under dark conditions with a maximum of 3 µW cm^{-2} and afterwards irradiated with a constant energy of 0.72 J cm^{-2}.

20 µl of the reaction were transferred into 180 µl Mueller Hinton bouillon after irradiation and cultivated at 37°C for 48 h. Optical density was measured at 600 nm using a plate reader. The obtained values were then used to calculate bacterial reduction as described elsewhere [59]. The method presented here was initially described as proliferation assay [60] and was adapted in the here presented study for liquid bacterial cultures. Doubling times were calculated for OD_{600} at 0.2 and 0.4.

2.8. Binding assays

To exclude interactions hindering photosensitizer attachment to bacterial cells, the bacterial cell suspensions were initially adjusted to an optical density of 0.6 at 600 nm. 500 µl thereof were transferred into 1.5 ml reaction tubes, centrifuged, and washed in water as described before. The washed pellet was mixed with 500 µl of the ionic solution and 500 µl of PS in a concentration of 100 µmol l^{-1}. The mixture was incubated for 10 min in absolute darkness and centrifuged at 4,500 x g for 10 min. The supernatant was collected and transferred into a cuvette and measured at 444 nm for FLASH-06a, 446 nm for FLASH-02a, 370 nm for SAPYR, 520 nm for TMPyP and 575 nm for MB.

3. Results

3.1. Photostability

Photosensitizers dissolved in H_2O did not show alterations in the transmission spectra after application of up to 5.4 J cm^{-2} radiant exposure, only a marginal loss of concentration of the photosensitizer was observed. (Supplementary Figure 1, Supplementary File 1). The transmission spectra for photosensitizers dissolved in 75 mmol l^{-1} $CaCl_2$ were also not altered after irradiation besides minor concentration losses (Supplementary Figure 2, Supplementary File 2). The concentration decreased in similar amounts as for the water controls. Photosensitizers dissolved in $MgCl_2$ solutions again showed low photodegradation not exceeding 2 % compared to the non-irradiated controls. Also, the photosensitizers maintained their chemical integrity (Supplementary Figure 3, Supplementary File 3), except for TMPyP as a bathochromic shift was observed. The transmission minimum (Soret band) was shifted to 435 nm and the Q bands were located at 520 to 521 and at 562 to 564 (Fig 1, Supplementary File 3).

3.2. Singlet oxygen production

As mentioned before, singlet oxygen production was measured as relative fluorescence of DPBF. The data are additionally given as a table in Supplementary File 4. Lower relative fluorescence hints at more efficient singlet oxygen production while values above 1 are measured, when the photobleaching effect of the reference exceeds the loss of the fluorescence caused by the photosensitizer. Relative fluorescence of DPBF for MB decreased at 10 µmol l^{-1} already to values around 0.2 for H_2O and $MgCl_2$ solution, while the same relative fluorescence value was achieved for $CaCl_2$ solution at the highest concentration of PS applied (Fig 2).

DPBF assays of TMPyP showed already drastically lowered relative fluorescence for 1 µmol l^{-1} of TMPyP. Application of concentrations as low as 5µmol l^{-1} of TMPyP already led to a relative fluorescence of around 0.1, indicating that all DPBF present in the reaction was readily depleted in all cases independent of the used solvents (Supplementary Figure 4B).

DPBF assays for SAPYR (Supplementary Figure 4C), FLASH-02a (Supplementary Figure 4D) and FLASH-06a (Supplementary Figure 4E) showed a similar reduction of the relative fluorescence mostly independent of the used solvents reaching minimal values of 0.1 to 0.2 for 50 µmol l^{-1} of applied PS.

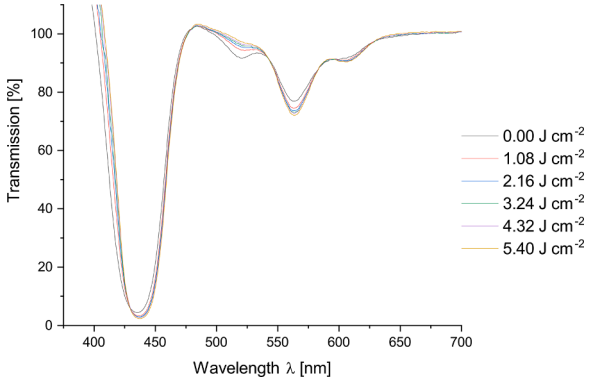

Fig. 1. Transmission spectrum of TMPyP resuspended in 75 mmol l^{-1} $MgCl_2$. The Y-axis indicates the transmission in %, the X-axis displays the corresponding wavelength in nm. The different line colors indicate the applied fluences.

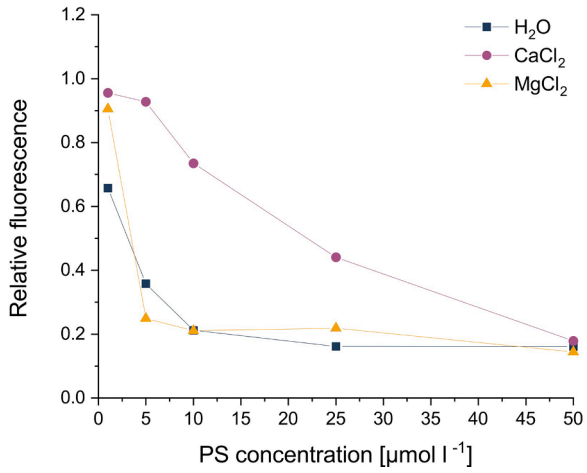

Fig. 2. Results of DPBF assays for MB.
Relative fluorescence is displayed on the Y-axis in dependence of the photosensitizer concentration shown on the X-axis in µmol l^{-1}. Blue lines and squares indicate H_2O as solvents, purple lines and dots $CaCl_2$ and yellow lines and triangles indicate $MgCl_2$.

3.3. Binding assays

MB showed good binding behavior towards *S. aureus* cells in the presence of H_2O. However, the binding efficiency decreased with increasing ion concentration (Fig 3A). The measured concentrations for *S. aureus* are also given as a table in Supplementary File 5. The use of TMPyP showed a comparable but less pronounced effect (Fig 3B). The binding of SAPYR (Fig 3C), FLASH-02a (Fig 3D) and FLASH-06a (Fig 3E) was almost unaltered in the presence of divalent ions.

The highest amounts of bound PS were measured for FLASH-02a with or without 0.75 mmol l^{-1} $MgCl_2$ showing around 96 µmol l^{-1} or 95 µmol l^{-1}, respectively. MB bound with 86 µmol l^{-1} to *S. aureus* cells in the case of H_2O as a maximum value, followed by TMPyP with 81 µmol l^{-1} for H_2O. Most SAPYR was bound for the application of H_2O with 78 µmol l^{-1} and the least amount of PS was found for FLASH-06a with 76 µmol l^{-1} for 0.75 mmol l^{-1} $CaCl_2$ not differing significantly from the other measured values for the other experimental conditions.

The measured concentrations for *P. aeruginosa* are additionally displayed in Supplementary File 6 as a table. Again, MB bound well to *P. aeruginosa* cells in the presence of H_2O. As shown for *S. aureus*, $CaCl_2$ and $MgCl_2$ solutions inhibited the binding of MB to the cells drastically (Fig 4A). Descending ionic concentrations led to higher amounts of bound photosensitizer. Furthermore, TMPyP (Fig 4B) showed a similar effect but only in insignificant amounts. As observed for MRSA, the binding of SAPYR (Fig 4C), FLASH-02a (Fig 4D) and FLASH-06a (Fig 4E) did not change in the presence of $CaCl_2$ and $MgCl_2$ solutions. FLASH-02a showed the most PS bound to the cells with 97 µmol l^{-1} for 0.75 mmol l^{-1} $MgCl_2$ with minor fluctuations for the other applied ionic solutions indicating that nearly all used PS bound to the cells. The concentration of MB in the presence of H_2O was measured with 90 µmol l^{-1} and for TMPyP 85 µmol l^{-1}. SAPYR and FLASH-06a showed similar binding behavior with a maximum of 78 µmol l^{-1} for SAPYR in H_2O and 77 µmol l^{-1} for FLASH-06a in H_2O, respectively.

3.4. PDI of Pseudomonas aeruginosa

The mean logarithmic reduction values for *P. aeruginosa* resuspended in $CaCl_2$ are additionally provided as table in Supplementary File 7. PDI at 0.72 J cm^{-2} for MB in H_2O led to bacterial reduction of at least 6 log_{10} steps at a PS concentration as low as 10 µmol l^{-1}. 0.75 mmol l^{-1} $CaCl_2$ inhibited the PDI of MB and the PDI effect almost disappeared (< 1 log_{10}

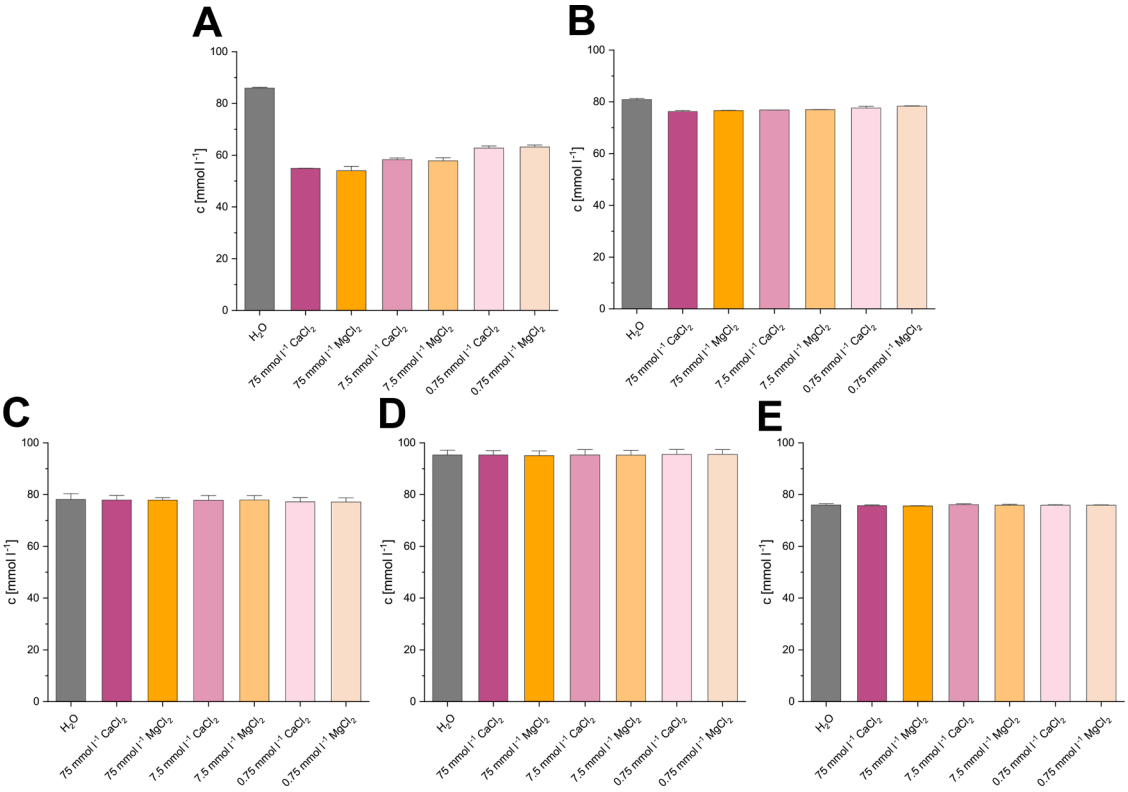

Fig. 3. Binding assays of *Staphylococcus aureus*.
The graphs show the bound concentration of the PS to MRSA cells for (A) MB, (B) TMPyP, (C) SAPYR, (D) FLASH-02a and (E) FLASH-06a. The X-axis displays the various tested categories named accordingly, the Y-axis indicates the concentration of PS bound to MRSA cells in µmol l^{-1}. Error bars were calculated as standard error.

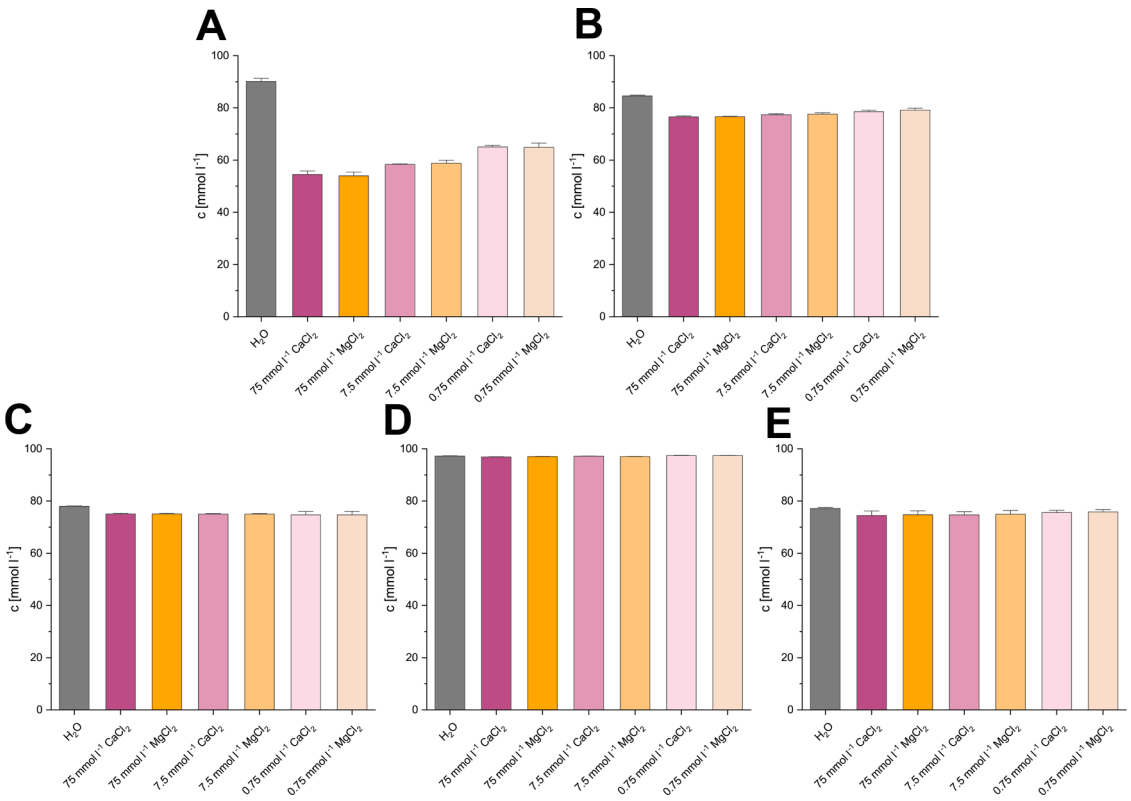

Fig. 4. Binding assays of *Pseudomonas aeruginosa*.
The graphs show the bound concentration of the PS to *P. aeruginosa* cells for (A) MB, (B) TMPyP, (C) SAPYR, (D) FLASH-02a and (E) FLASH-06a. The X-axis displays the various tested categories named accordingly, the Y-axis indicates the concentration of PS bound to MRSA cells in μmol l^{-1}. Error bars were calculated as standard error.

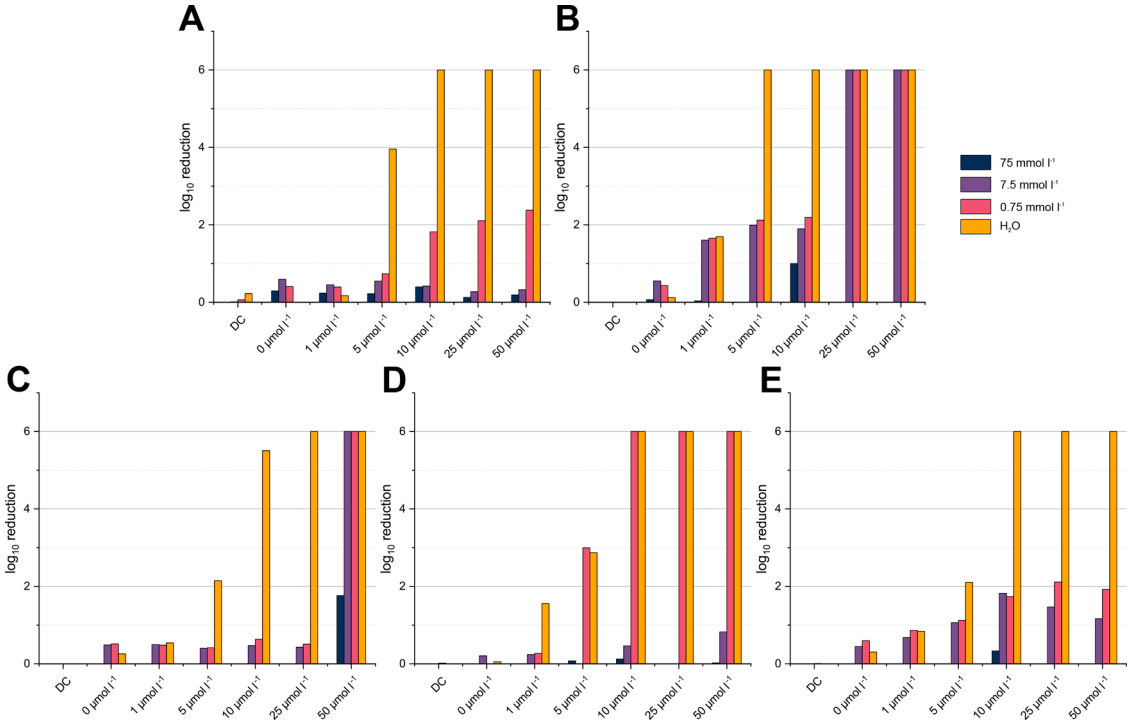

Fig. 5. Diagrams of the calculated logarithmic reduction of *Pseudomonas aeruginosa* resuspended in $CaCl_2$ solutions in different concentrations.
The logarithmic reduction is displayed on the Y-axis while the dark control (DC) and applied PS concentrations are displayed on the X-axis. The different concentrations of the ions are symbolized by various colors indicated in the right corner. Panels A shows results for MB, B for TMPyP, C for SAPYR, D for FLASH-02a, E for FLASH-06a.

step) for concentrations of 75 or 7.5 mmol l^{-1} $CaCl_2$ (Fig 5A). In H_2O 5 µmol l^{-1} TMPyP and above led to a bacterial reduction of 6 log_{10} steps. $CaCl_2$ inhibited the photodynamic mechanism for 5 and 10 µmol l^{-1} as only a logarithmic reduction around 2 log_{10} steps was measured for 7.5 and 0.75 mmol l^{-1} $CaCl_2$. However, in none of the cases for 75 mmol l^{-1} $CaCl_2$ the efficacy exceeded 1 log_{10} step (Fig 5B). The application of SAPYR led to an efficient inactivation at concentrations as low as 10 µmol l^{-1} in H_2O. For 75 mmol l^{-1} $CaCl_2$ (Fig 5C) almost no bacterial reduction was observed. Lower concentrations of $CaCl_2$ led to an inactivation of 6 log_{10} steps for the application of 50 µmol l^{-1} SAPYR. 10 µmol l^{-1} FLASH-02a and above led to an inactivation of 6 log_{10} steps (Fig 5D). Addition of 75 or 7.5 mmol l^{-1} $CaCl_2$ led to no efficient inactivation when FLASH-02a was applied under mentioned conditions, only 0.75 mmol l^{-1} showed similar efficacy to the water control (Fig 5D). In H_2O, concentrations of 10 µmol l^{-1} FLASH-06a and above yielded an efficacy of 6 log_{10} steps. The application of $CaCl_2$ did not lead to a reduction that exceeded 2 log_{10} steps in any cases (Fig 5E).

A table of the mean logarithmic reduction of *P. aeruginosa* resuspended $MgCl_2$ is provided in Supplementary File 8. The application of $MgCl_2$ had slightly less inhibitory effects on the PDI with MB (Fig 6A) than $CaCl_2$. Results obtained for TMPyP with bacteria resuspended in $MgCl_2$ solutions (Fig 6B) did not differ much from the beforehand presented results for $CaCl_2$. The application of 50 µmol l^{-1} SAPYR in 75 mmol l^{-1} $MgCl_2$ led to a maximum bacterial reduction of about 1 log_{10} step. Lower $MgCl_2$ concentrations led to a maximum inactivation of around 4 log_{10} steps for 7.5 mmol l^{-1} $MgCl_2$ and 6 log_{10} steps for 0.75 mmol l^{-1} $MgCl_2$, respectively (Fig 6C). *P. aeruginosa* suspended in 7.5 mmol $MgCl_2$ solution were inactivated with an efficacy not exceeding 1 log_{10} step, 0.75 mmol l^{-1} $MgCl_2$ solution showed a bacterial reduction of around 4 log_{10} steps for 50 µmol l^{-1} FLASH-02a. 6 log_{10} steps were observed for 25 µmol l^{-1} FLASH-02a and above in 0.75 mmol l^{-1} $MgCl_2$ (Fig 6D). The experimental outcome of the application of $MgCl_2$ in combination with FLASH-06a showed a slightly higher inactivation efficacy for 75 mmol l^{-1} compared to $CaCl_2$. However, for 7.5 mmol l^{-1} $MgCl_2$ the efficacy did not exceed 2 log_{10} steps. 0.75 mmol l^{-1} $MgCl_2$ restored an efficacy of 6 log_{10} steps for 25 and 50 µmol l^{-1} FLASH-06a (Fig 6E).

3.5. PDI of Staphylococcus aureus

Additionally, to the mentioned experiments with *P. aeruginosa*, the same set of conditions were tested for a methicillin resistant *S. aureus* strain (MRSA). A tabular presentation of the results is provided in Supplementary File 9. The application of MB in H_2O led to an efficacy of 6 log_{10} steps for 25 and 50 µmol l^{-1}. 5 and 10 µmol l^{-1} led to an efficacy < 3 log_{10} steps (Fig 7A). In general, inactivation in the presence of $CaCl_2$ solution did not show any relevant reduction for 1 µmol l^{-1}. The application of 5 µmol l^{-1} MB showed a reduction < 2 log_{10} steps for 0.75 mmol l^{-1} $CaCl_2$. For 10 µmol l^{-1} MB, the application of 7.5 mmol l^{-1} $CaCl_2$ led to an efficacy of 3.5 log_{10} steps. 0.75 mmol l^{-1} $CaCl_2$ showed a reduction for 10 µmol l^{-1} MB with 3.1 log_{10} steps. 25 µmol l^{-1} MB achieved for 7.5 mmol l^{-1} $CaCl_2$ an efficacy of around 3 log_{10} steps at most. 50 µmol l^{-1} MB did not increase the efficacy for 75 and 7.5 mmol l^{-1} $CaCl_2$ while the application of 0.75 mmol l^{-1} $CaCl_2$ showed an efficacy of 6 log_{10} steps (Fig 7 A). The photosensitizer TMPyP showed excellent efficacy in H_2O for 10 µmol l^{-1} and above with an efficacy 6 log_{10} steps (Fig 7B). 75 mmol l^{-1} $CaCl_2$ did not lead to efficient inactivation, 7.5 mmol l^{-1} $CaCl_2$ solution showed a reduction of 1.3 log_{10} steps for 5 µmol l^{-1} and 6 log_{10} steps for 10 µmol l^{-1} and above. Application of 0.75 mmol l^{-1} $CaCl_2$ showed better efficacy compared to the water control for 1 and 5 µmol l^{-1} TMPyP. 25 and 50 µmol l^{-1} restored the efficacy of the PDI with 6 log_{10} steps. (Fig 7B). SAYPR in H_2O was capable of an inactivation of 6 log_{10} steps for 25 µmol l^{-1} and above. However, the application of 75 mmol l^{-1} $CaCl_2$ led to no noteworthy reduction in bacterial viability (Fig 7C). The water control of FLASH-02a showed a reduction of 6 log_{10} steps for 25 and 50 µmol l^{-1} (Fig 7D), only minor efficacy was achieved for lower concentrations. However, when $CaCl_2$ solutions were applied, in none of the applied

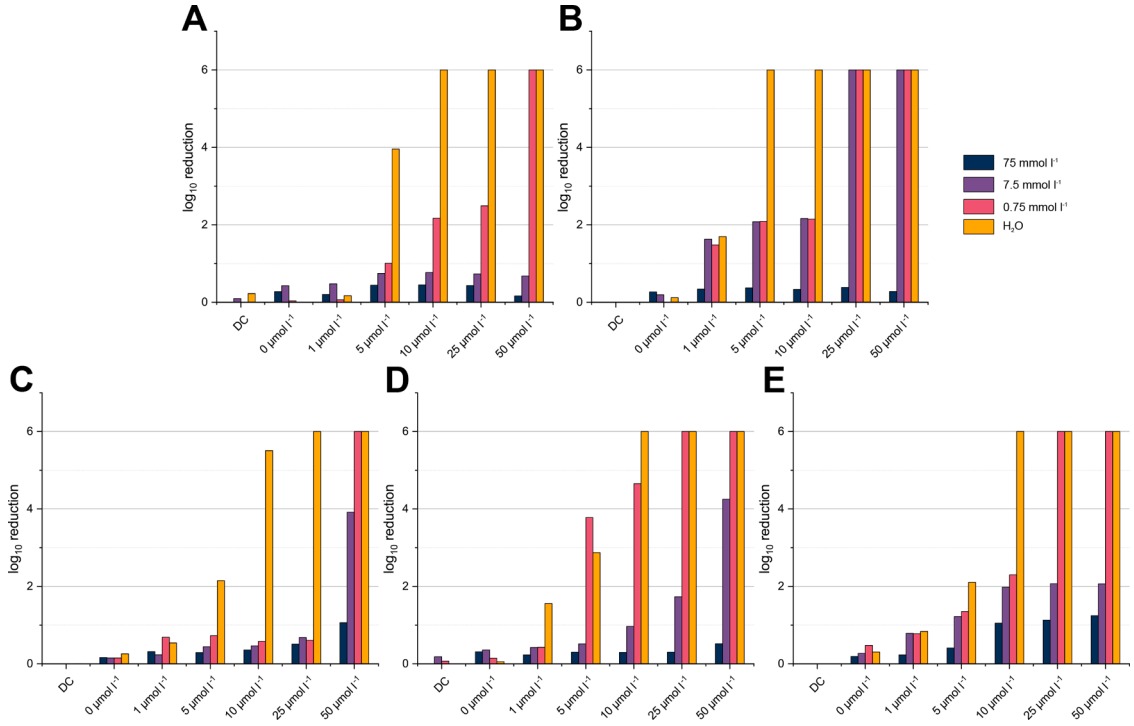

Fig. 6. Diagrams of the calculated logarithmic reduction of *Pseudomonas aeruginosa* resuspended in $MgCl_2$ solutions in different concentrations.
The logarithmic reduction is displayed on the Y-axis while the dark control (DC) and applied PS concentrations are displayed on the X-axis. The different concentrations of the ions are symbolized by various colors indicated in the right corner. Panels A shows results for MB, B for TMPyP, C for SAPYR, D for FLASH-02a, E for FLASH-06a.

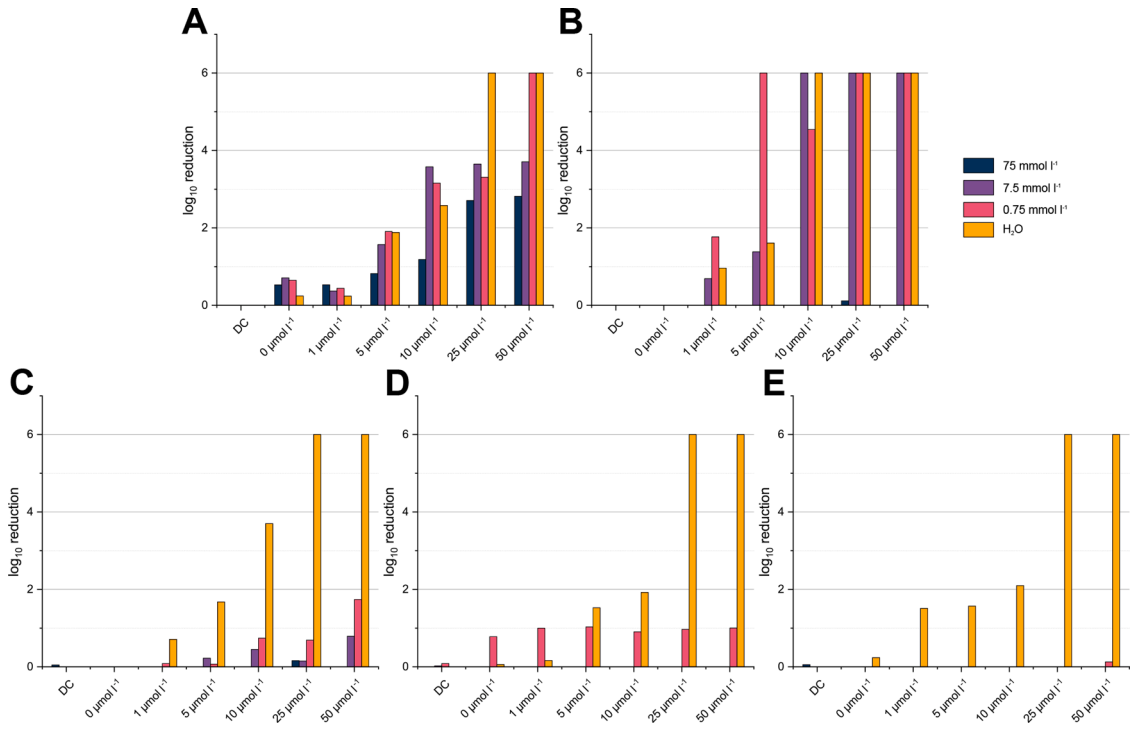

Fig. 7. Diagrams of the calculated logarithmic reduction of *Staphylococcus aureus* resuspended in $CaCl_2$ solutions in different concentrations.
The logarithmic reduction is displayed on the Y-axis while the dark control (DC) and applied PS concentrations are displayed on the X-axis. The different concentrations of the ions are symbolized by various colors indicated in the right corner. Panels A shows results for MB, B for TMPyP, C for SAPYR, D for FLASH-02a, E for FLASH-06a.

concentrations a noteworthy reduction was achieved (Fig 7D). While the water control for FLASH-06a (Fig 7E) did not differ in significant manners from the data for FLASH-02a, the addition of $CaCl_2$ aggravates the problems even more, no measurable reduction could be achieved (Fig 7E).

The obtained results for S. aureus resuspended in $MgCl_2$ are also

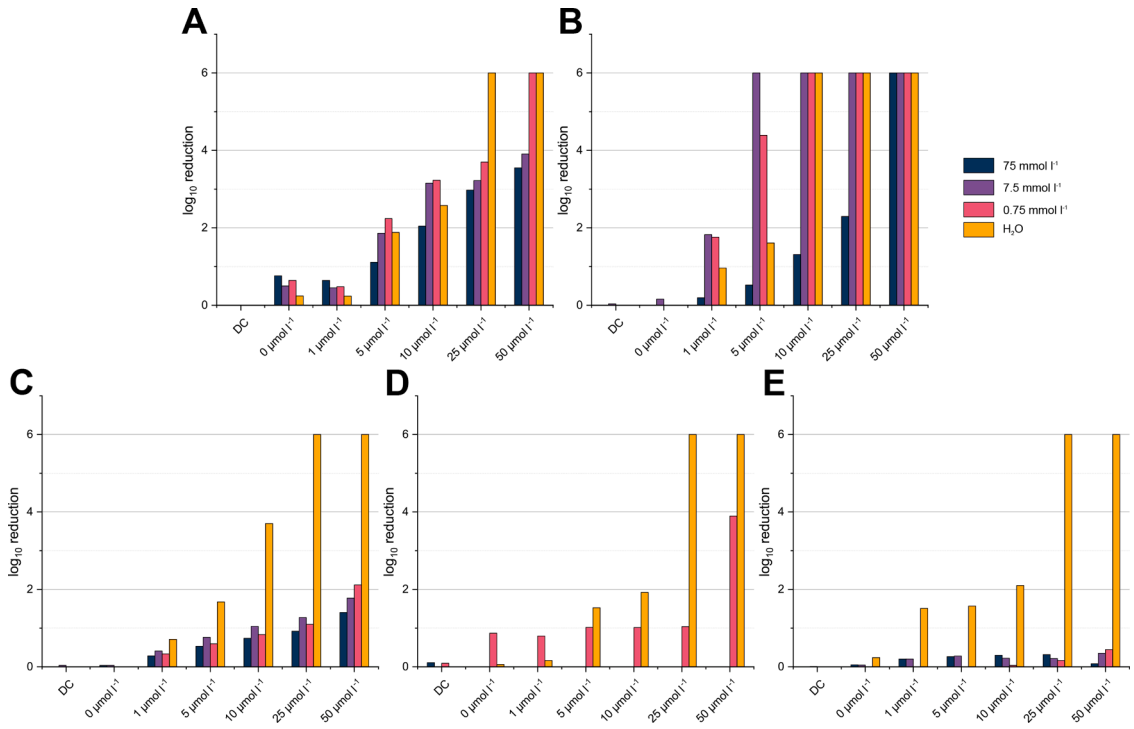

Fig. 8. Diagrams of the calculated logarithmic reduction of *Staphylococcus aureus* resuspended in $MgCl_2$ solutions in different concentrations.
The logarithmic reduction is displayed on the Y-axis while the dark control (DC) and applied PS concentrations are displayed on the X-axis. The different concentrations of the ions are symbolized by various colors indicated in the right corner. Panels A shows results for MB, B for TMPyP, C for SAPYR, D for FLASH-02a, E for FLASH-06a.

displayed as a table in Supplementary File 10. MB in the presence of $MgCl_2$ solutions had mediocre inactivation efficacy between 2 and 4 log_{10} steps for 5 to 25 μmol l^{-1} MB. 6 log_{10} steps of bacterial reduction were achieved for 0.75 mmol l^{-1} $MgCl_2$ for the highest applied MB concentration (Fig 8A). *S. aureus* resuspended in $MgCl_2$ solutions with TMPyP led to a good overall efficacy as 6 log_{10} steps were achieved even for the highest $MgCl_2$ concentration applied (Fig 8B). For the application of $MgCl_2$ solution in combination with SAPYR the maximum efficacy obtained was around 2 log_{10} steps for the highest SAPYR concentration (Fig 8C). Most dramatically influenced by the application of $MgCl_2$ were both FLASH-06a and FLASH-02a. For FLASH-02a, the only mentionable observed reduction was that at least for 0.75 mmol l^{-1} $MgCl_2$ at a concentration of 50 μmol l^{-1} FLASH-02a a reduction of around 4 log_{10} steps (Fig 8D). FLASH-06a in combination with $MgCl_2$ solutions led to no relevant observable reduction (Fig 8E).

4. Discussion

The presented results paint quite a clear picture concerning the role of $CaCl_2$ and $MgCl_2$ when performing PDI against the bacteria and photosensitizers used. Firstly, the absorption spectra showed that all photosensitizers in pure water were stable upon irradiation with up to 5.4 J/cm^2. Even the addition of the divalent ions at different concentrations showed no negative effect on photostability of photosensitizers, except for TMPyP in the presence of $MgCl_2$ (Fig 1). This is not surprising because a porphyrin structure is a pristine chelating agent for divalent ions [61]. The fact that the complexation of bivalent metal ions causes alterations in the spectrum of porphyrins has been described in literature before [62–64]. However, such chelating reactions of the porphyrin group are often influenced by specific reaction parameters such as defined pH [65–67] or temperatures [68,69]. This might also lead to incomplete complexation reactions, which could also be influenced upon light exposure explaining the different transmission spectra after irradiation. Further possible explanations of this change in absorption behavior in the Q bands might be potential partial cleavage of the methylpyrimidinum groups of TMPyP especially as the side chains of porphyrins seem to rather influence the absorption of the Q bands than of the Soret band [70,71]. The DPBF assays showed an efficient generation of singlet oxygen by all photosensitizers in combination with both divalent ions, except for MB in the presence of $CaCl_2$ (Fig 2). It seems that singlet oxygen production of TMPyP is even at 1 μmol l^{-1} due to its high absorption coefficient so efficient that the relative fluorescence of DPBF dropped by nearly 0.5 for H_2O or even more for $CaCl_2$ and $MgCl_2$ solutions (Supplementary Figure 2B). However, quantitative conclusions concerning the DPBF assays involving TMPyP are limited as both excitation and emission wavelength of DPBF match those of TMPyP to a certain extent. With the TMPyP concentrations applied here it is likely that most photons are absorbed by TMPyP, therefore a concentration dependent comparison of the relative fluorescence should be treated with caution.

These two exceptions might not automatically reduce the efficacy of PDI. TMPyP has a rather high extinction coefficient [72] that even low amounts of functional PS can lead to efficient inactivation which is also reflected by the shown results for the biological inactivation as TMPyP showed the best inactivation efficacy under the given experimental conditions. It is also known that TMPyP with complexed metals is still capable of singlet oxygen production [41]. One of the possible explanations is that the complexation reaction might not be a process that takes place for all TMPyP molecules. Further, a change in pH value in the adjacency of bacterial cells might have stopped or even reverted the complexation.

In most of the PDI applications, the generation of singlet oxygen plays the major role in cell killing [73]. However, the photosensitizers may have the potential to generate not only singlet oxygen, as proven by DPBF assays in the present study. SAPYR shows a singlet oxygen quantum yield with a value of $\Phi_\Delta = 0.99$ [20], TMPyP $\Phi_\Delta = 0.77$ [74], the flavins $\Phi_\Delta = 0.75$ to 0.78 [75], and MB $\Phi_\Delta = 0.52$ [76]. In particular, the Φ_Δ of MB could allow a simultaneous generation of other reactive oxygen species (ROS) that may also yield cell killing. A fact one should keep in mind is especially the potential photodemethylation of diaminomethylgroups as observed for example for photosensitizers like nocathoacin I [77] or methylene blue [78]. For the case of methylene blue, a degradation occurs to azure a or b, leading to reduced singlet oxygen yields and the potential increase of type I reactions [76,79]. However, it seems that calcium and magnesium ions do not favor such demethylation processes in an excessive manner as there are no hints that the spectra of the herein used methylene blue are altered in such ways.

At a glance, the microbial inactivation data, in the absence of the ions, showed an efficient PDI of all tested photosensitizers with a respective concentration of 25 μmol l^{-1} yielding a reduction of 6 log_{10} steps at low radiant exposure of light (Figs 5-8). Except for TMPyP, the efficacy of all photosensitizers is clearly lower in the presence of elevated concentrations of calcium and magnesium ions (Figs 5-8). A general observable trend was that increased concentrations of $CaCl_2$ and $MgCl_2$ led to inhibited inactivation. The effects were most severe for the tested flavins which are also affected by other ions such as carbonate or phosphate [21].

The applied concentrations of $CaCl_2$ and $MgCl_2$ resemble the concentrations present in several fields of application.The two lower $CaCl_2$ concentrations applied within this work, namely 7.5 and 0.75 mmol l^{-1} cover the usual calcium concentration in tap water [25–33]. Within this mentioned ranges, TMPyP is most efficient against Gram-negatives, followed by SAPYR and FLASH-02a. However, the findings in this study leads to an exclusion of FLASH-06a and MB from its potential use in such water applications. Gram-positives seem to be mostly inhibited by TMPyP again, but now followed by MB. SAPYR and the flavin based PS did not yield sufficient efficacy under the influence of calcium and magnesium ions. However, concerning drinking water applications, Gram-negatives such as *Shigella* sp., *Vibrio* sp., *Salmonella* sp. or *Escherichia coli* are the more crucial organisms as one of the main causes of contaminated drinking water [80].

The concentrations of magnesium ions usually present in drinking water [34–40] suggest that the magnesium ions poses less of a problem compared to calcium ion concentrations. Especially Gram-negatives might be readily inactivated in magnesium concentrations below 0.75 mmol l^{-1}.

Concerning food applications, potential use in dairy products are the most crucial applications in the light of the herein presented results due to their elevated calcium content [44–47]. Based on the results of this work, the use of TMPyP might show sufficient success concerning the reduction of the bacterial load while the other PS used here seem to be less promising. However, a publication already observed reduced efficacy of applied PDI and the authors speculated that calcium and magnesium might take a part in the reduced efficacy besides further substances such as proteins or fatty acids [44].

Many researchers have already reported that the outermost layers of bacteria seem to be the target of PDI or at least play a major role in the uptake of the PS. A study by George, Hamblin and Kishen from 2009 revealed for MB that the PS showed lower uptake in the presence of divalent ions [81]. Although this study confirms the findings concerning MB, the other PS show no relevant difference in their uptake or binding behavior. Therefore, the sole differences in uptake and binding behavior of the PS do not explain the drastic differences observed in the microbial efficacy. Concerning cationic photosensitizers it is highly likely that negatively charged LPS molecules in the outer membrane that need calcium and magnesium ions for stability [82] form a positively charged layer surrounding the cell that electrostatically hinder the penetration of the PS up to the outer membrane but bind to outer sugar moieties of the LPS. Especially the fact that ions have a stabilizing effect has been reviewed extensively concerning the use of EDTA [83]. Further, this stability hypothesis is strengthened by a study demonstrating a

efficacy-promoting effect of EDTA with zinc phthalocyanine against Gram-negative cells, which are without EDTA not effected by negatively or neutrally charged photosensitizers [84]. Similar might be true for Gram-positive cells as teichoic acids and wall teichoic acids have a certain metal ion binding capacity [85–87]. However, these calcium and magnesium ion interactions seem to be not fully understood yet [87].

5. Conclusion

Although the divalent ions calcium and magnesium have no direct effects on the investigated PS such as chemical degradation their levels for an application in PDI must be kept as low as possible. Therefore, appropriate dilution of the treated liquids or rinsing of surfaces like the human skin with distilled water prior to PDI treatment is highly recommended for future research. Furthermore, several suggestions for the application of photodynamic processes can be given: First, based on several studies that were performed under various conditions, it becomes clear that increased light intensity helps to overcome inhibitory processes, even those of calcium or magnesium ions. Second, higher PS concentrations seem to support the PDI in general. Under these predictions, PDI is an extremely promising antimicrobial treatment for the future, independently on the type of microorganisms or their antibiotic resistances.

Funding

This work was funded by the Deutsche Forschungsgemeinschaft (DFG, German Research Foundation) – Projektnummer 415812443

Declaration of Competing Interest

The authors declare the following financial interests/personal relationships which may be considered as potential competing interests:

Harald Huber reports financial support was provided by German Research Foundation. Wolfgang Baeumler reports financial support was provided by German Research Foundation.

Acknowledgement

We thank G. Gmeinwieser for technical assistance as well as L. Nißl for conducting preliminary experiments.

Supplementary materials

Supplementary material associated with this article can be found, in the online version, at doi:10.1016/j.jpap.2022.100122.

References

[1] J. Almeida, J.P.C. Tomé, M.G.P.M.S. Neves, A.C. Tomé, J.A.S. Cavaleiro, Â. Cunha, L. Costa, M.A.F. Faustino, A. Almeida, Photodynamic inactivation of multidrug-resistant bacteria in hospital wastewaters: Influence of residual antibiotics, Photochem. Photobiol. Sci. 13 (2014) 626–633, https://doi.org/10.1039/c3pp50195g.

[2] C.M.B. Carvalho, A.T.P.C. Gomes, S.C.D. Fernandes, A.C.B. Prata, M.A. Almeida, M. A. Cunha, J.P.C. Tomé, M.A.F. Faustino, M.G.P.M.S. Neves, A.C. Tomé, J.A. S. Cavaleiro, Z. Lin, J.P. Rainho, J. Rocha, Photoinactivation of bacteria in wastewater by porphyrins: Bacterial β-galactosidase activity and leucine-uptake as methods to monitor the process, J. Photochem. Photobiol. B Biol. 88 (2007) 112–118, https://doi.org/10.1016/j.jphotobiol.2007.04.015.

[3] M. Jemli, Z. Alouini, S. Sabbahi, M. Gueddari, Destruction of fecal bacteria in wastewater by three photosensitizers, J. Environ. Monit. 4 (2002) 511–516, https://doi.org/10.1039/b204637g.

[4] G. Jori, M. Magaraggia, C. Fabris, M. Soncin, M. Camerin, L. Tallandini, O. Coppellotti, L. Guidolin, Photodynamic inactivation of microbial pathogens: Disinfection of water and prevention of water-borne diseases, J. Environ. Pathol. Toxicol. Oncol. 30 (2011) 261–271, https://doi.org/10.1615/JEnvironPatholToxicolOncol.v30.i3.90.

[5] R.J. Watts, S. Kong, M.P. Orr, G.C. Miller, B.E. Henry, Photocatalytic inactivation of coliform bacteria and viruses in secondary wastewater effluent, Water Res 29 (1995) 95–100, https://doi.org/10.1016/0043-1354(94)E0122-M.

[6] M. Bartolomeu, C. Oliveira, C. Pereira, M.G.P.M.S. Neves, M.A.F. Faustino, A. Almeida, Antimicrobial Photodynamic Approach in the Inactivation of Viruses in Wastewater: Influence of Alternative Adjuvants, Antibiot 10 (2021), https://doi.org/10.3390/antibiotics10070767.

[7] M. Bartolomeu, S. Reis, M. Fontes, M.G.P.M.S. Neves, M.A.F. Faustino, A. Almeida, Photodynamic Action against Wastewater Microorganisms and Chemical Pollutants: An Effective Approach with Low Environmental Impact, Water 9 (2017), https://doi.org/10.3390/w9090630.

[8] C.P. Gerba, C. Wallis, J.L. Melnick, Disinfection of Wastewater by Photodynamic Oxidation, J. (Water Pollut. Control Fed. 49 (1977) 575–583. http://www.jstor.org/stable/25039316.

[9] A. Eichner, T. Holzmann, D.B. Eckl, F. Zeman, M. Koller, M. Huber, S. Pemmerl, W. Schneider-Barchert, W. Bäumler, Novel photodynamic coatings reduce the bioburden on near-patient surface thereby reducing the risk for onward pathogen transmission – a field study in two hospitals, J. Hosp. Infect. 104 (2020) 85–91, https://doi.org/10.1016/j.jhin.2019.07.016.

[10] M.R.E. Santos, P.V Mendonça, R. Branco, R. Sousa, C. Dias, A.C. Serra, J. R. Fernandes, F.D. Magalhães, P.V Morais, J.F.J. Coelho, Light-Activated Antimicrobial Surfaces Using Industrial Varnish Formulations to Mitigate the Incidence of Nosocomial Infections, ACS Appl. Mater. Interfaces. 13 (2021) 7567–7579, https://doi.org/10.1021/acsami.0c18930.

[11] T.Q. Corrêa, K.C. Blanco, É.B. Garcia, S.M.L. Perez, D.J. Chianfrone, V.S. Morais, V. S. Bagnato, Effects of ultraviolet light and curcumin-mediated photodynamic inactivation on microbiological food safety: A study in meat and fruit, Photodiagnosis Photodyn. Ther. 30 (2020), 101678, https://doi.org/10.1016/j.pdpdt.2020.101678.

[12] M. Glueck, B. Schamberger, P. Eckl, K. Plaetzer, New horizons in microbiological food safety: Photodynamic Decontamination based on a curcumin derivative, Photochem. Photobiol. Sci. 16 (2017) 1784–1791, https://doi.org/10.1039/c7pp00165g.

[13] M. Glueck, C. Hamminger, M. Fefer, J. Liu, K. Plaetzer, Save the crop: Photodynamic Inactivation of plant pathogens I: Bacteria, Photochem. Photobiol. Sci. 18 (2019) 1700–1708, https://doi.org/10.1039/c9pp00128j.

[14] C.B. Penha, E. Bonin, A.F. da Silva, N. Hioka, É.B. Zanqueta, T.U. Nakamura, B. A. de Abreu Filho, P.A.Z. Campanerut-Sá, J.M.G. Mikcha, Photodynamic inactivation of foodborne and food spoilage bacteria by curcumin, LWT - Food Sci. Technol. 76 (2017) 198–202, https://doi.org/10.1016/j.lwt.2016.07.037.

[15] M. Schreiner, W. Bäumler, D.B. Eckl, A. Späth, B. König, A. Eichner, Photodynamic inactivation of bacteria to decolonize meticillin-resistant *Staphylococcus aureus* from human skin, Br. J. Dermatol. 179 (2018) 1358–1367, https://doi.org/10.1111/bjd.17152.

[16] F. Foschi, C.R. Fontana, K. Ruggiero, R. Riahi, A. Vera, A.G. Doukas, T.C. Pagonis, R. Kent, P.P. Stashenko, N.S. Soukos, Photodynamic inactivation of Enterococcus faecalis in dental root canals in vitro, Lasers Surg. Med. 39 (2007) 782–787, https://doi.org/10.1002/lsm.20579.

[17] F. Cieplik, A. Pummer, C. Leibl, J. Regensburger, G. Schmalz, W. Buchalla, K.-A. Hiller, T. Maisch, Photodynamic Inactivation of Root Canal Bacteria by Light Activation through Human Dental Hard and Simulated Surrounding Tissue, Front. Microbiol. 7 (2016) 929. https://www.frontiersin.org/article/10.3389/fmicb.2016.00929.

[18] C. Santezi, J.M.G. Tanomaru, V.S. Bagnato, O.B.O. Júnior, L.N. Dovigo, Potential of curcumin-mediated photodynamic inactivation to reduce oral colonization, Photodiagnosis Photodyn. Ther. 15 (2016) 46–52, https://doi.org/10.1016/j.pdpdt.2016.04.006.

[19] H. Majiya, K.F. Chowdhury, N.J. Stonehouse, P. Millner, TMPyP functionalised chitosan membrane for efficient sunlight driven water disinfection, J. Water Process Eng. 30 (2019), 100475, https://doi.org/10.1016/j.jwpe.2017.08.013.

[20] F. Cieplik, A. Späth, J. Regensburger, A. Gollmer, L. Tabenski, K.A. Hiller, W. Bäumler, T. Maisch, G. Schmalz, Photodynamic biofilm inactivation by SAPYR - An exclusive singlet oxygen photosensitizer, Free Radic. Biol. Med. 65 (2013) 477–487, https://doi.org/10.1016/j.freeradbiomed.2013.07.031.

[21] D.B. Eckl, S.S. Eben, L. Schottenhaml, A. Eichner, R. Vasold, A. Späth, W. Bäumler, H. Huber, Interplay of phosphate and carbonate ions with flavin photosensitizers in photodynamic inactivation of bacteria, PLoS One 16 (2021), e0253212, https://doi.org/10.1371/journal.pone.0253212.

[22] N.A. Kuznetsova, O.L. Kaliya, Photodynamic water disinfection, Russ. J. Gen. Chem. 85 (2015) 321–332, https://doi.org/10.1134/S1070363215010466.

[23] M. Magaraggia, G. Jori, Photodynamic approaches to water disinfection. CRC Handb. Org. Photochem. Photobiol, Third Ed., CRC Press, 2019, pp. 1543–1556. Vol. Set.

[24] A. Lesar, G. Begić, N. Malatesti, I. Gobin, Innovative approach in *Legionella* water treatment with photodynamic cationic amphiphilic porphyrin, Water Supply 19 (2019) 1473–1479, https://doi.org/10.2166/ws.2019.012.

[25] USGS, Hardness of Water, (n.d.).

[26] Gesetz über die Umweltverträglichkeit von Wasch- und Reinigungsmitteln, Bundesgesetzblatt 1 (2013) 2539–2542.

[27] H. Sjörs, U. Gunnarsson, Calcium and pH in north and central Swedish mire waters, J. Ecol. 90 (2002) 650–657, https://doi.org/10.1046/j.1365-2745.2002.00701.x.

[28] A. Azoulay, P. Garzon, M.J. Eisenberg, Comparison of the mineral content of tap water and bottled waters, J. Gen. Intern. Med. 16 (2001) 168–175, https://doi.org/10.1111/j.1525-1497.2001.04189.x.

[29] A.A. Olajire, F.E. Imeokparia, Water Quality Assessment of Osun River: Studies on Inorganic Nutrients, Environ. Monit. Assess. 69 (2001) 17–28, https://doi.org/10.1023/A:1010796410829.

[30] J. Cotruvo, J. Bartram, Calcium and Magnesium in Drinking-water, Public health significance, Geneva, 2009. :.

[31] A. Kumar, D. Roberts, K.E. Wood, B. Light, J.E. Parrillo, S. Sharma, R. Suppes, D. Feinstein, S. Zanotti, L. Taiberg, D. Gurka, A. Kumar, M. Cheang, Duration of hypotension before initiation of effective antimicrobial therapy is the critical determinant of survival in human septic shock, Crit. Care Med. 34 (2006) 1589–1596, https://doi.org/10.1097/01.CCM.0000217961.75225.E9.

[32] M. Kumar, S. Singh, R.K. Mahajan, Trace Level Determination of U, Zn, Cd, Pb and Cu in Drinking Water Samples, Environ. Monit. Assess. 112 (2006) 283–292, https://doi.org/10.1007/s10661-006-1069-6.

[33] I. Al-Saleh, I. Al-Doush, Survey of trace elements in household and bottled drinking water samples collected in Riyadh, Saudi Arabia, Sci. Total Environ. 216 (1998) 181–192, https://doi.org/10.1016/S0048-9697(98)00137-5.

[34] R. Rylander, H. Bonevik, E. Rubenowitz, Magnesium and calcium in drinking water and cardiovascular mortality, Scand. J. Work. Environ. Health. 17 (1991) 91–94. http://www.jstor.org/stable/40965866.

[35] E. Rubenowitz, G. Axelsson, R. Rylander, Magnesium in drinking water and body magnesium status measured using an oral loading test, Scand, J. Clin. Lab. Invest. 58 (1998) 423–428, https://doi.org/10.1080/00365519850186409.

[36] E. Rubenowitz, G. Axelsson, R. Rylander, Magnesium in drinking water and death from acute myocardial infarction, Am. J. Epidemiol. 143 (1996) 456–462.

[37] T.P. Flaten, B. Bølviken, Geographical associations between drinking water chemistry and the mortality and morbidity of cancer and some other diseases in Norway, Sci. Total Environ. 102 (1991) 75–100.

[38] T. Peder Flaten, A nation-wide survey of the chemical composition of drinking water in Norway, Sci. Total Environ. 102 (1991) 35–73, https://doi.org/10.1016/0048-9697(91)90307-Z.

[39] R. Maheswaran, S. Morris, S. Falconer, A. Grossinho, I. Perry, J. Wakefield, P. Elliott, Magnesium in drinking water supplies and mortality from acute myocardial infarction in north west England, Heart 82 (1999), https://doi.org/10.1136/hrt.82.4.455, 455 LP –460.

[40] W.P. Leary, AJ Reyes, CJ Lockett, DD Arbuckle, K van der Byl, Magnesium and deaths ascribed to ischaemic heart disease in South Africa-a preliminary report, South African Med. J. 64 (1983) 775–776.

[41] J. Tang, G. Tang, J. Niu, J. Yang, Z. Zhou, Y. Gao, X. Chen, Y. Tian, Y. Li, J. Li, Y. Cao, Preparation of a Porphyrin Metal–Organic Framework with Desirable Photodynamic Antimicrobial Activity for Sustainable Plant Disease Management, J. Agric. Food Chem. 69 (2021) 2382–2391, https://doi.org/10.1021/acs.jafc.0c06487.

[42] V. Jesus, D. Martins, T. Branco, N. Valério, M.G.P.M.S. Neves, M.A.F. Faustino, L. Reis, E. Barreal, P.P. Gallego, A. Almeida, An insight into the photodynamic approach versus copper formulations in the control of Pseudomonas syringae pv. actinidiae in kiwi plants, Photochem. Photobiol. Sci. 17 (2018) 180–191, https://doi.org/10.1039/C7PP00300E.

[43] D. Martins, M.Q. Mesquita, M.G.P.M.S. Neves, M.A.F. Faustino, L. Reis, E. Figueira, A. Almeida, Photoinactivation of Pseudomonas syringae pv. actinidiae in kiwifruit plants by cationic porphyrins, Planta 248 (2018) 409–421, https://doi.org/10.1007/s00425-018-2913-y.

[44] A. Galstyan, U. Dobrindt, Determining and unravelling origins of reduced photoinactivation efficacy of bacteria in milk, J. Photochem. Photobiol. B Biol. (2019) 197, https://doi.org/10.1016/j.jphotobiol.2019.111554.

[45] T.V Armstrong, Variations in the Gross Composition of Milk as Related to the Breed of the Cow: A Review and Critical Evaluation of Literature of the United States and Canada1, J. Dairy Sci. 42 (1959) 1–19, https://doi.org/10.3168/jds.S0022-0302(59)90518-1.

[46] J.W. Hibbs, Principles of dairy chemistry (Jenness, Robert; Patton, Stuart), J. Chem. Educ 37 (1960) 274, https://doi.org/10.1021/ed037p274.4.

[47] P. Posati, L. Linda, Orr Martha, Composition of Foods - Dairy and Egg Products - Raw - Processed - Prepared, United States Department of Agriculture, Washington, DC, 1976.

[48] X. Ragàs, T. Dai, G.P. Tegos, M. Agut, S. Nonell, M.R. Hamblin, Photodynamic inactivation of *Acinetobacter baumannii* using phenothiazinium dyes: *In vitro* and *in vivo* studies, Lasers Surg. Med. 42 (2010) 384–390, https://doi.org/10.1002/lsm.20922.

[49] S. ROBINSON, A.H. ROBINSON, Chemical composition of sweat, Physiol. Rev. 34 (1954) 202–220, https://doi.org/10.1152/physrev.1954.34.2.202.

[50] K.G. FOSTER, Relation between the colligative properties and chemical composition of sweat, J. Physiol. 155 (1961) 490–497, https://doi.org/10.1113/jphysiol.1961.sp006641.

[51] F. Wilkinson, W.P. Helman, A.B. Ross, Rate Constants for the Decay and Reactions of the Lowest Electronically Excited Singlet State of Molecular Oxygen in Solution. An Expanded and Revised Compilation, J. Phys. Chem. Ref. Data. 24 (1995) 663–677, https://doi.org/10.1063/1.555965.

[52] L. Yuan, P. Lyu, Y.Y. Huang, N. Du, W. Qi, M.R. Hamblin, Y. Wang, Potassium iodide enhances the photobactericidal effect of methylene blue on *Enterococcus faecalis* as planktonic cells and as biofilm infection in teeth, J. Photochem. Photobiol. B Biol. 203 (2020), 111730, https://doi.org/10.1016/j.jphotobiol.2019.111730.

[53] L. Huang, G. Szewczyk, T. Sarna, M.R. Hamblin, Potassium Iodide Potentiates Broad-Spectrum Antimicrobial Photodynamic Inactivation Using Photofrin, ACS Infect. Dis. 3 (2017) 320–328, https://doi.org/10.1021/acsinfecdis.7b00004.

[54] L. Huang, T.G. St. Denis, Y. Xuan, Y.Y. Huang, M. Tanaka, A. Zadlo, T. Sarna, M. R. Hamblin, Paradoxical potentiation of methylene blue-mediated antimicrobial photodynamic inactivation by sodium azide: Role of ambient oxygen and azide radicals, Free Radic, Biol. Med. 53 (2012) 2062–2071, https://doi.org/10.1016/j.freeradbiomed.2012.09.006.

[55] R.W. Redmond, J.N. Gamlin, A Compilation of Singlet Oxygen Yields from Biologically Relevant Molecules, Photochem. Photobiol. 70 (1999) 391–475, https://doi.org/10.1111/j.1751-1097.1999.tb08240.x.

[56] F. Wilkinson, W.P. Helman, A.B. Ross, Quantum Yields for the Photosensitized Formation of the Lowest Electronically Excited Singlet State of Molecular Oxygen in Solution, J. Phys. Chem. Ref. Data. 22 (1993) 113–262, https://doi.org/10.1063/1.555934.

[57] D.B. Eckl, L. Dengler, M. Nemmert, A. Eichner, W. Bäumler, H. Huber, A Closer Look at Dark Toxicity of the Photosensitizer TMPyP in Bacteria, Photochem Photobiol. (n.d.).

[58] J.H. Mueller, J. Hinton, A Protein-Free Medium for Primary Isolation of the *Gonoeceus* and *Meningococcus*, Proc. Soc. Exp. Biol. Med. 48 (1941) 330–333, https://doi.org/10.3181/00379727-48-13311.

[59] D.B. Eckl, H. Huber, W. Bäumler, First Report on Photodynamic Inactivation of Archaea Including a Novel Method for High-Throughput Reduction Measurement, Photochem. Photobiol. 96 (2020) 883–889, https://doi.org/10.1111/php.13229.

[60] T. Bechert, P. Steinrücke, J.P. Guggenbichler, A new method for screening anti-infective biomaterials, Nat. Med. 6 (2000) 1053–1056, https://doi.org/10.1038/79568.

[61] M. Zamadar, C. Orr, M. Uherek, Water Soluble Cationic Porphyrin Sensor for Detection of Hg^{2+}, Pb^{2+}, Cd^{2+}, and Cu^{2+}, J. Sensors. 2016 (2016), 1905454 https://doi.org/10.1155/2016/1905454.

[62] J. Li, Y. Wei, L. Guo, C. Zhang, Y. Jiao, S. Shuang, C. Dong, Study on spectroscopic characterization of Cu porphyrin/Co porphyrin and their interactions with ctDNA, Talanta 76 (2008) 34–39, https://doi.org/10.1016/j.talanta.2008.01.065.

[63] S. Igarashi, H. Suzuki, T. Yotsuyanagi, The equilibrium constants of cadmium (II)-, lead (II)-, magnesium (II)-, and zinc (II)-α, β, γ, δ-tetrakis (1-methylpyridinium-4-yl) porphine complexes, Talanta 42 (1995) 1171–1177.

[64] M. Gouterman, Spectra of porphyrins, J. Mol. Spectrosc 6 (1961) 138–163, https://doi.org/10.1016/0022-2852(61)90236-3.

[65] L. Di Costanzo, S. Geremia, L. Randaccio, R. Purrello, R. Lauceri, D. Sciotto, F. G. Gulino, V. Pavone, Calixarene–Porphyrin Supramolecular Complexes: pH-Tuning of the Complex Stoichiometry, Angew, Chemie Int. Ed. 40 (2001) 4245–4247, https://doi.org/10.1002/1521-3773(20011119)40:22<4245::AID-ANIE4245>3.0.CO;2-#.

[66] M. Wolak, R. van Eldik, pH Controls the Rate and Mechanism of Nitrosylation of Water-Soluble FeIII Porphyrin Complexes, J. Am. Chem. Soc. 127 (2005) 13312–13315, https://doi.org/10.1021/ja052855n.

[67] E.B. Fleischer, E.I. Choi, P. Hambright, A. Stone, Porphyrin studies: kinetics of metalloporphyrin formation, Inorg. Chem. 3 (1964) 1284–1287.

[68] W.S. Caughey, R.M. Deal, B.D. McLees, J.O. Alben, Species equilibria in nickel (II) porphyrin solutions: Effect of porphyrin structure, solvent and temperature, J. Am. Chem. Soc. 84 (1962) 1735–1736.

[69] J. Seth, V. Palaniappan, D.F. Bocian, Oxidation of nickel (II) tetraphenylporphyrin revisited. Characterization of stable nickel (III) complexes at room temperature, Inorg. Chem 34 (1995) 2201–2206.

[70] D. Lazzeri, M. Rovera, L. Pascual, E.N. Durantini, Photodynamic Studies and Photoinactivation of *Escherichia coli* Using meso-Substituted Cationic Porphyrin Derivatives with Asymmetric Charge Distribution, Photochem. Photobiol. 80 (2004) 286–293, https://doi.org/10.1562/2004-03-08-ra-105.1.

[71] P.G. Mahajan, N.C. Dige, B.D. Vanjare, A.R. Phull, S.J. Kim, S.-K. Hong, K.H. Lee, Synthesis, photophysical properties and application of new porphyrin derivatives for use in photodynamic therapy and cell imaging, J. Fluoresc. 28 (2018) 871–882.

[72] R.F. Pasternack, P.R. Huber, P. Boyd, G. Engasser, L. Francesconi, E. Gibbs, P. Fasella, G. Cerio Venturo, L. deC. Hinds, Aggregation of meso-substituted water-soluble porphyrins, J. Am. Chem. Soc. 94 (1972) 4511–4517, https://doi.org/10.1021/ja00768a016.

[73] M. Wainwright, T. Maisch, S. Nonell, K. Plaetzer, A. Almeida, G.P. Tegos, M. R. Hamblin, Photoantimicrobials—are we afraid of the light? Lancet Infect. Dis. 17 (2017) e49–e55.

[74] P.K. Frederiksen, S.P. McIlroy, C.B. Nielsen, L. Nikolajsen, E. Skovsen, M. Jørgensen, K.V Mikkelsen, P.R. Ogilby, Two-Photon Photosensitized Production of Singlet Oxygen in Water, J. Am. Chem. Soc. 127 (2005) 255–269, https://doi.org/10.1021/ja0452020.

[75] T. Maisch, A. Eichner, A. Späth, A. Gollmer, B. König, J. Regensburger, W. Bäumler, Fast and effective photodynamic inactivation of multiresistant bacteria by cationic riboflavin derivatives, PLoS One 9 (2014), e111792, https://doi.org/10.1371/journal.pone.0111792.

[76] Y. Usui, K. Kamogawa, A STANDARD SYSTEM TO DETERMINE THE QUANTUM YIELD OF SINGLET OXYGEN FORMATION IN AQUEOUS SOLUTION, Photochem. Photobiol. 19 (1974).

[77] W. Li, S. Huang, X. Liu, J.E. Leet, J.L. Cantone, K.S. Lam, N-Demethylation of nocathiacin I via photo-oxidation, Bioorg. Med. Chem. Lett. 18 (2008) 4051–4053, https://doi.org/10.1016/j.bmcl.2008.05.112.

[78] T. Zhang, T. ki Oyama, S. Horikoshi, H. Hidaka, J. Zhao, N. Serpone, Photocatalyzed N-demethylation and degradation of methylene blue in titania dispersions exposed to concentrated sunlight, Sol. Energy Mater. Sol. Cells. 73 (2002) 287–303, https://doi.org/10.1016/S0927-0248(01)00215-X.

[79] K. Hirakawa, Fluorometry of singlet oxygen generated via a photosensitized reaction using folic acid and methotrexate, Anal. Bioanal. Chem. 393 (2009) 999–1005, https://doi.org/10.1007/s00216-008-2522-x.

[80] J.P.S. Cabral, Water microbiology. Bacterial pathogens and water, Int. J. Environ. Res. Public Health. 7 (2010) 3657–3703, https://doi.org/10.3390/ijerph7103657.

[81] S. George, M.R. Hamblin, A. Kishen, Uptake pathways of anionic and cationic photosensitizers into bacteria, Photochem. Photobiol. Sci. 8 (2009) 788–795, https://doi.org/10.1039/b809624d.

[82] R.E.W. Hancock, ALTERATIONS IN OUTER MEMBRANE PERMEABILITY, Annu. Rev. Microbiol 38 (1984) 237–264, https://doi.org/10.1146/annurev.mi.38.100184.001321.
[83] S. Finnegan, S.L. Percival, EDTA: An Antimicrobial and Antibiofilm Agent for Use in Wound Care, Adv. Wound Care. 4 (2014) 415–421, https://doi.org/10.1089/wound.2014.0577.
[84] G. Bertolini, F. Rossi, G. Valduga, G. Jori, J. Van Lier, Photosensitizing activity of water- and lipid-soluble phthalocyanines on *Escherichia coli*, FEMS Microbiol. Lett. 71 (1990) 149–155, https://doi.org/10.1111/j.1574-6968.1990.tb03814.x.
[85] R.J. Doyle, T.H. Matthews, U.N. Streips, Chemical basis for selectivity of metal ions by the Bacillus subtilis cell wall, J. Bacteriol. 143 (1980) 471–480, https://doi.org/10.1128/jb.143.1.471-480.1980.
[86] N. Yee, D.A. Fowle, F.G. Ferris, A Donnan potential model for metal sorption onto Bacillus subtilis, Geochim. Cosmochim. Acta. 68 (2004) 3657–3664.
[87] K.J. Thomas 3rd, C.V Rice, Revised model of calcium and magnesium binding to the bacterial cell wall, Biometals 27 (2014) 1361–1370, https://doi.org/10.1007/s10534-014-9797-5.